Solid-State Modification of Isotactic Polypropylene (iPP) via Grafting of Styrene. II. Morphology and Melt Processing

F. Picchioni,[1,*] J. G. P. Goossens,[1] M. van Duin[2]

[1]*Dutch Polymer Institute, Department of Polymer Technology (SKT), Eindhoven University of Technology, P.O. Box 513, 5600 MB, Eindhoven, The Netherlands*
[2]*DSM Research, P.O. Box 18, 6160 MD Geleen, The Netherlands*

Received 29 July 2003; accepted 27 April 2004
DOI 10.1002/app.21015
Published online in Wiley InterScience (www.interscience.wiley.com).

ABSTRACT: Grafting of vinyl monomers onto isotactic polypropylene (iPP) in the solid state represents a convenient route to chemically modify iPP and, consequently, its properties. Solid-state modification can be carried out on iPP powder directly from the polymerization reactor. The modified powder is then processed in the melt, usually with the addition of fillers and/or additives, to obtain the final product. In this work we have studied the effect of melt processing on the morphology of solid-state polymerized PP/polystyrene (PS) blends, i.e., of a iPP powder previously modified in the solid-state with styrene (St) and optionally in the presence of divinylbenzene (DVB). A series of samples containing different amounts of PS and displaying different grafting efficiencies were investigated before and after processing in the melt. Transmission electron microscopy, scanning electron microscopy, and solid-state NMR were used to investigate the morphology on different length scales. It was shown that PS coalescence during processing can be hindered, thereby stabilizing the initially polymerized iPP/PS blends morphology. Indeed, reducing the PS amount in the blend or increasing the grafting efficiency resulted in less coalescence of the PS domains. Crosslinking of the PS phase during the solid-state polymerization resulted also in a very fine but heterogeneous morphology. © 2005 Wiley Periodicals, Inc. J Appl Polym Sci 97: 575–583, 2005

Key words: polystyrene; polypropylene; solid state; blends; morphology

INTRODUCTION

The main advantage of carrying out grafting of isotactic polypropylene (iPP) in the solid state (at temperatures close to 100°C) is that the degradation of iPP via β-scission reaction, which takes place extensively when iPP is processed in the melt, can be neglected.[1,2] As a result, the modified iPP practically retains its original molecular weight.

Modification of iPP in the solid state is the basis of an industrial process developed by Montell in the early 1990s, which resulted in the commercialization of the Hivalloy products.[3–13] The process consists of grafting vinyl monomers onto porous iPP powder at temperatures below the iPP melting point, usually in the range between 90 and 125°C.[11] The grafting reaction is mostly carried out with monomers that homopolymerize under the employed experimental conditions. As a result a new polymeric phase is formed upon polymerization, i.e., a polymer blend is formed. The final properties of the obtained blend are dependent on the chemical nature of the new polymer phase and on its dispersion into the PP matrix. Assuming that the starting iPP powder particles are actually composed of several microparticles (multigrain model),[5,6] it is then possible to investigate the spatial distribution of the newly formed polymeric phase in the iPP particles.[14,15] For iPP modified with styrene a distinction could be made between the PS present on the surface of the macroparticle and PS that is inside the macroparticle. The relative amount of these two kinds of PS can be tuned by adjusting the ratio between the polymerization and diffusion rates.[14]

The use of styrene as a monomer in the solid-state modification of iPP has been widely investigated,[16–20] leading to the development of an industrial process for the production of grafted iPP-*g*-PS materials containing about 20 wt % of PS with an average grafting efficiency of 50%, i.e., half of the PS is grafted onto PP. The process can simply be carried out in a batch mixer as well as in a fluidized bed reactor. The working temperature should be selected on the basis of diffusion studies of the components into the PP grains. The possibility of a chemical control of the grafting efficiency, that is of the ratio between grafted and ho-

Correspondence to: F. Picchioni (f.picchioni@chem.rug.nl).
**Present address*: Product Engineering, Stratingh Institute, University of Groningen, Nijenborgh 4, 9747 AG Groningen, The Netherlands.

mopolymerized chains, in the case of the styrene grafting onto iPP was recently[21] reported.

From the previously mentioned studies it may be evident that the solid-state grafting polymerization can be easily controlled to achieve the desired grafting efficiency and particle morphology. However, very little is known, at least in the open literature, about the influence of these parameters on the morphology during the subsequent melt-processing step. The stability of the morphology upon melting seems to constitute a key issue. Phase-inversion phenomena have been reported[22] to take place when processing a polymerized iPP/PS blend. This phase inversion is due to the fact that, in the starting material, PS, being polymerized on the surface of the iPP particle, forms a kind of continous network/matrix. During melt processing, PP, which is in weight and volume excess with respect to PS, becomes the matrix. The author suggested that upon melt processing the morphology may be stable or not depending on the grafting efficiency but no experimental data were presented.

In this work the processing of polymerized iPP/PS blends is studied with respect to the stability of the morphology. Samples characterized by different grafting efficiency values have been processed in the melt and the resulting morphology compared to that of physical iPP/PS blends, i.e., of blends obtained by simply mixing iPP and PS in the melt.

EXPERIMENTAL

Materials

iPP (M_n = 400,000, M_w/M_n = 2.9) was kindly supplied by DSM Research (Geleen, The Netherlands). It is in the form of a white powder (particle diameter of approximately 0.3 mm) and displays a DSC crystallinity of about 51 wt % at 90°C (reaction temperature).

Styrene (St, Aldrich) and divinylbenzene (DVB, Aldrich) containing 10–15 ppm of a radical inhibitor (4-*tert*-butylcatechol) were used without further purification. Chlorobenzene (Merck), *n*-octane (Aldrich), and dichloromethane (CH_2Cl_2, Merck) were used without further purification. The free radical initiator, 2,2′-azobis(2-methylpropionitrile) (AIBN, Merck), was used as received.

Grafting reactions

The grafting reactions were carried out in a typical solid-state,[23,24] double-skinned reactor preheated at 90°C, equipped with a condenser and a mechanical stirrer. The stirrer consists of a steel rod having at one edge a Teflon anchor perfectly fitting into the cylindrical shape of the reactor and, consequently, being able to remove scraps, whenever formed, from the reactor wall. The reactor was furthermore connected to a nitrogen inlet and a peristaltic pump by which the reactive mixture, St/AIBN/(DVB), was pumped into the reactor at the desired rate. The flow rate was calculated from the density of the reactive mixture, assumed to be approximately equal to the density of pure styrene, and the measured addition time. The flow rate is expressed, following the convention in the literature,[24] as pph/min: parts of reactive mixture per hundred parts of iPP per minute. The detailed description of the solid-state grafting experiments is given in the first paper of this series.[25]

TABLE I
Polymerized iPP/PS Blends

Blend	PS content (wt %)	ϕ (%)	Processing time (min)
iPPAH1	28 ± 1	30 ± 6	3
iPPAH2	28 ± 1	30 ± 6	15
iPPAH3	18 ± 2	94 ± 6	15
iPPAH4	3 ± 3	50 ± 6	15
iPPAH5[a]	28 ± 1[b]	n.d.	3
iPPAH6[a]	28 ± 1[b]	n.d.	15
iPPAH7[c]	28 ± 1[b]	n.d.	3
iPPAH8[c]	28 ± 1[b]	n.d.	15

[a] Obtained by polymerization of a 92/8 mol/mol St/DVB mixture in iPP.
[b] Under the assumption that the conversion does not change when DVB is copolymerized with St.
[c] Obtained by polymerization of a 99/1 mol/mol St/DVB mixture in iPP.

Processing in the melt

Processing of the polymerized iPP/PS blends was performed in a circulating, counterrotating, double-screw miniextruder at the temperature of 230°C. The screw speed was fixed at 100 rpm. The blends were introduced into the extruder chamber in approximately 30 s. After this point the chamber was sealed and the mixture was processed for the desired residence time, after which the circulation channel was reversed to recover the material. An overview of all studied blends is given in Table I together with the PS content and the grafting efficiency, which is defined by

$$\Phi = \frac{\text{amount of grafted PS (g)}}{\text{amount of total formed PS (g)}} \times 100 \quad (1)$$

The grafting efficiency for the polymerized blends containing DVB could not be measured due to the insolubility of the PS phase. The PS content was calculated on the basis of polymerized iPP/PS blends containing a similar amount of starting styrene.

Characterization techniques

Solid-state NMR

Proton-decoupled ^{13}C-NMR spectra were recorded on a Bruker DMX500 spectrometer operating at a ^{1}H- and

^{13}C-NMR frequency of 500 and 125 MHz, respectively. A 4-mm magic-angle-spinning (MAS) probehead was used with typical sample-rotation rates of 8 kHz. The radio-frequency power was adjusted to obtain a 5-μs 90° pulse both for ^{1}H and ^{13}C nuclei. Adamantane was used for external calibration of the ^{13}C chemical shift. Proton spin-lattice relaxation in the laboratory and rotating frame, T_1{H} and $T_{1\rho}${H}, were measured for each of the polymer components separately via cross-polarization to the ^{13}C nuclei. The typical number of scans (NS) was 256, relaxation delay (D1) was 5 s, and the number of experiments per relaxation data set (NE) was 12.

Scanning electron microscopy (SEM)

The morphology of the samples was visualized by Environmental Scanning Electron Microscopy (Philips XL30 FEG-ESEM xl30). Samples for E-SEM were cryogenically fractured and some were successively etched with toluene (15 min) to remove the free-PS phase.

Transmission electron microscopy (TEM)

TEM was performed using a Jeol JEM 2000 FX microscope operated at 80 kV. The starting material, i.e., the modified iPP powder, is composed of small spheres. They were embedded in Epofix at room temperature for microtoming. Since they tended to float, the embedding procedure was performed in two steps. After curing Epofix for 24 h, a sharp razorblade was used to cut a trapezium-shaped surface. Since the spheres are relatively large (0.3 mm) the surface consists completely of i-PP/PS. A diamond knife was used at low temperature (cryotrimming) to create an undeformed surface. For the processed samples, a simple cryotrimming procedure was used directly on the extrudate to obtain thin slices. The samples were then stained for 20 h in a ruthenium–tetraoxide (RuO_4) solution prepared according to the literature.[26] The PS was expected to be stained darker than the iPP phase.[27] Ultrathin sections were obtained using a Reichert Ultracut E microtome (wet cryomicrotomy).

Differential scanning calorimetry (DSC) analysis

Differential scanning calorimetry was performed on a Perkin–Elmer Pyris 1 DSC. Temperature calibration was performed with indium, hexatriacontane, and dodecane. Calibration of the heat of fusion was performed using the heat of fusion of indium. The baseline was obtained by performing a run with two empty pans using the same heating/cooling rate (10°C/min) as employed for the sample run. All samples were first heated from room temperature to 250°C (1st heat), immediately cooled down (1st cool) to room temperature and then heated up again to 250°C (2nd heat). All these operations were carried out at 10°C/min.

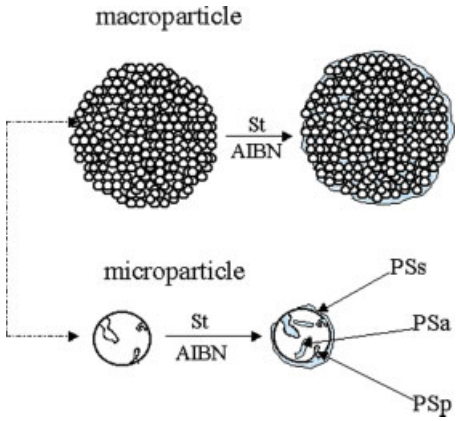

Figure 1 Polymerization of styrene in iPP particles (PSs, PS on the iPP microparticle surface; PSa, PS in the amorphous phase of iPP; PSp, PS in the iPP microparticle pores).

RESULTS AND DISCUSSION

Polymerization of styrene in the presence of solid iPP leads[25] to the formation of iPP/PS blends that display a spatial distribution of the PS phase in the PP particle. According to the multigrain model, every iPP particle is composed of several microparticles. As shown in Figure 1, styrene can polymerize on the surface of the PP microparticle (PSs), in the pores (PSp), and eventually, after absorption, in the amorphous phase of iPP (PSa). From a macroscopic point of view, it is noted that PSs can actually be present in the pores or at the surface of the macroparticle, depending on whether the corresponding microparticle is situated in the bulk or at the surface of the macroparticle.

The morphology of the polymerized iPP/PS blends before melt processing has been visualized by TEM (Fig. 2). The morphology of the blends is constituted by very small PS domains dispersed in the iPP matrix, in agreement with the polymerization behavior described in Figure 1. It is remarkable that the PS domains have dimensions ranging from 10 to 50 nm, i.e., the dispersion can undoubtedly be considered as nanoscopic. This morphology is the starting point to study the structural changes that may take place upon melt processing these materials.

Figure 3 displays the SEM images of iPPH1 and iPPH2, i.e., the morphology of the same polymerized iPP/PS blend of Figure 2 but after melt processing for 3 and 15 min, respectively. Several observations can be made. The morphology has dramatically changed upon processing: PS domains display now dimensions in the order of 1–10 μm. Extending the processing time beyond 3 min seems to have very little effect on the final morphology. This indicates that the equilibrium

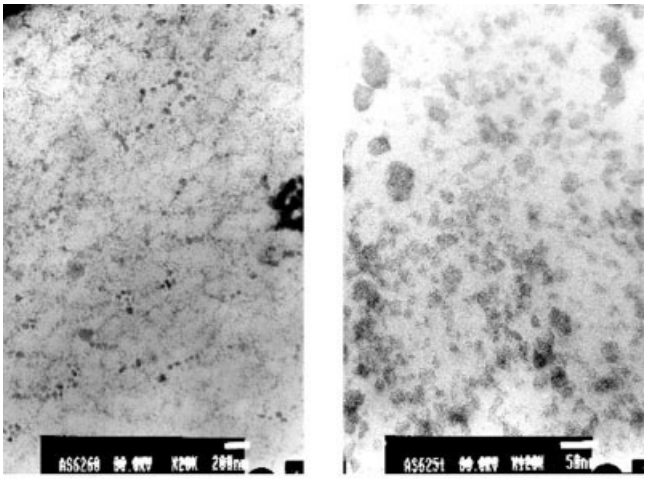

(a) (b)

Figure 2 TEM images of a polymerized iPP/PS blend (PS 28 wt %) before melt processing at different magnifications: scale bar 200 nm (a) and 50 nm (b).

morphology has already been attained before 3 min mixing time. Eventually, the morphology is comparable to that of physical, uncompatibilized iPP/PS blends (Fig. 4), which however display, at similar PS contents and processing conditions, a coarser structure characterized by PS domains size in the order of 10–20 μm.

These results clearly show that the morphology of the starting polymerized blend is not stable upon processing and that coalescence of the small PS domains takes place during melt processing. However, the final morphology still shows a finer PS dispersion in comparison to a physical PP/PS blend, probably because of the compatibilizing effect of the grafted copolymer (PP-*g*-PS) present in the polymerized blends.

It is possible to obtain an even finer morphology if the coalescence during processing is somehow hindered. One possible way to accomplish this is to decrease the PS content of the starting material since the frequency of PS particles "collisions" is obviously decreased. Large PS aggregates are not observed in the SEM picture (Fig. 5) of sample iPPAH4 (3 wt % PS), indicating that coalescence is reduced during processing. The same kind of observation can be made for iPPAH3 (Fig. 6), a sample with a high grafting efficiency, which also does not display the presence of PS aggregates in the micrometer scale. However, this fact does not mean that coalescence is completely avoided. Indeed the TEM image (Fig. 7) clearly shows, apart for

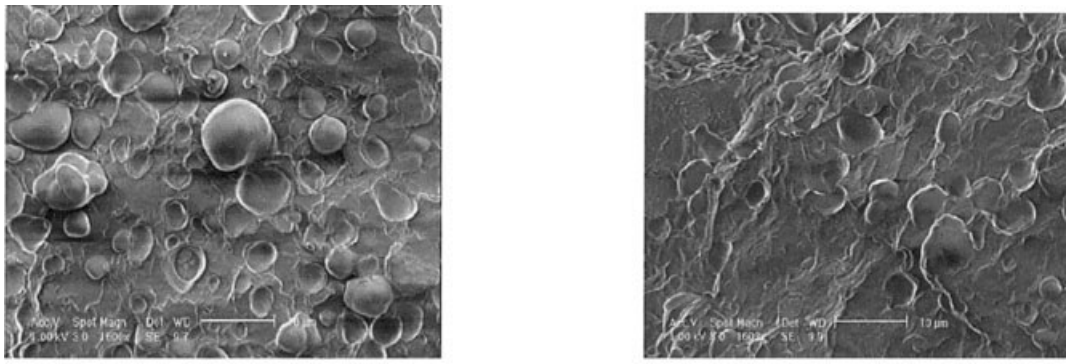

(a) (b)

Figure 3 SEM images of iPPAH1 (a) and iPPAH2 (b, etched with toluene); 28 wt % PS, Φ = 30%.

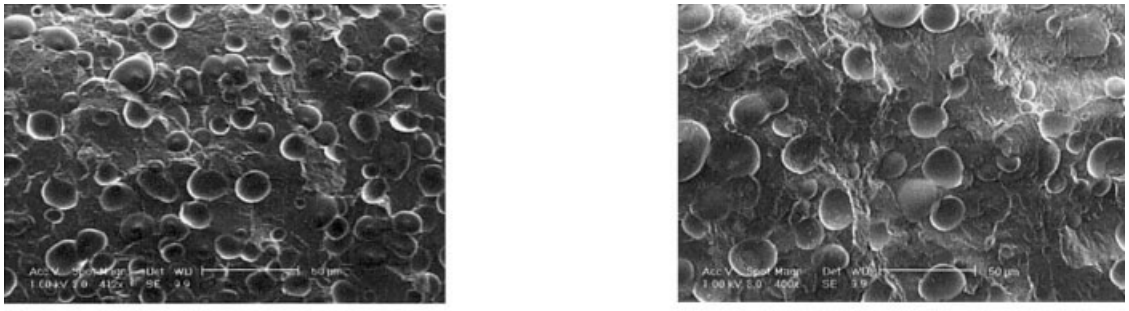

(a) (b)

Figure 4 SEM images of physical iPP/PS blends (PS 30 wt %): iPP/PS 70/30 processed for 3 min at 230°C (scale bar 50 μm) (a) and iPP/PS 70/30 processed for 15 min at 230°C (scale bar 50 μm) (b).

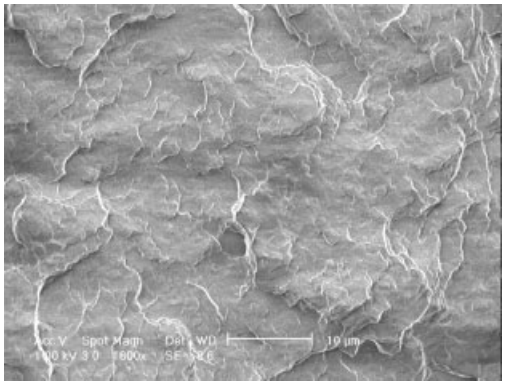

Figure 5 SEM image of iPPAH4 (3 wt % PS, Φ = 50%); scale bar 10 μm.

small domains of about 50 nm (i.e., the same size observed before melt processing), the presence of PS domains, whose size is in the order of 300 nm. This clearly indicates that the morphology is not completely stable since coalescence causes a small increase in the PS domains size. Furthermore it must be outlined that some PS domains fully retain their original dimensions upon processing. This fact is also confirmed by the TEM image of iPPAH1 (Fig. 8), which shows the presence of PS domains larger than 500 nm and of small ones of about 50 nm. These results can be partially explained, according to what was suggested in the literature,[22] by assuming that the grafted PS chains form smaller PS domains, while free PS forms the larger ones.

Both the SEM and TEM pictures give a very "local" overview of the morphology; this is due to the fact that both kinds of techniques focus necessarily only on a relatively small region of the sample. A more accurate definition of the morphology can in general be achieved by combining the TEM and SEM results with

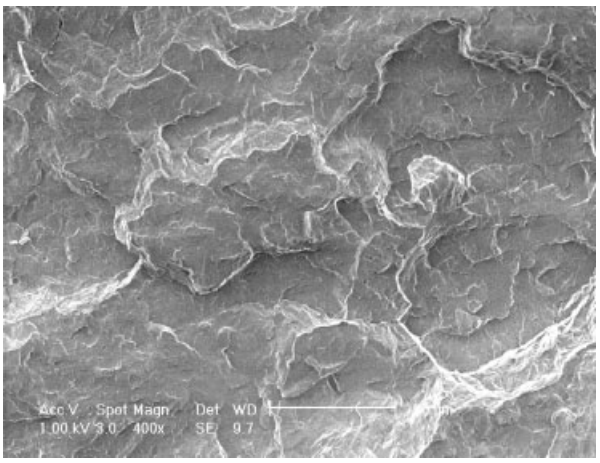

Figure 6 SEM image of iPPAH3 (18 wt % PS, Φ = 94%); scale bar 50 μm.

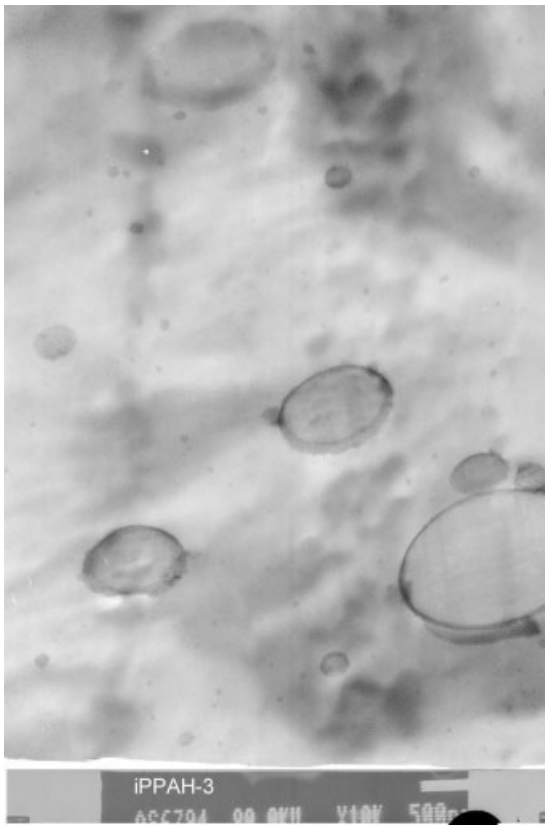

Figure 7 TEM micrograph of iPPAH3 (18 wt % PS, Φ = 94%); scale bar 500 nm.

solid-state NMR[28,29] experiments, since the later technique provides a more general picture of the domain size. In Table II are displayed the values of the relaxation times, both in the laboratory (T_1) and rotating frame ($T_{1\rho}$), for PS and PP in the samples iPPAH2 and iPPAH3 before and after processing (an example of the recorded NMR spectra is reported in Fig. 9). For comparison a physical blend iPPA/PS 70/30 has been also investigated. Several points are worth mentioning. The T_1 and $T_{1\rho}$ values for the PP and PS phases are significantly different in the physical iPP/PS blend and are very close to the values observed for the pure components, clearly indicating that the two components are phase separated in the micrometer scale with sharp phase boundaries. In the iPPAH2 sample before processing, the T_1 values are close to each other while the $T_{1\rho}$ values remain appreciably different. It can be concluded that in the polymerized blends the PS phase is more intimately mixed with the PP phase than in normal melt-processed samples. After processing iPPAH2, the T_1 values for iPP and PS diverge, suggesting that a phase coarsening has taken place. In the iPPAH3 sample before melt processing, the T_1 values are rather close to each other, while the $T_{1\rho}$ values are clearly different. This indicates that the two components in the starting polymerized blend are separated on the nanometer scale. Processing does not

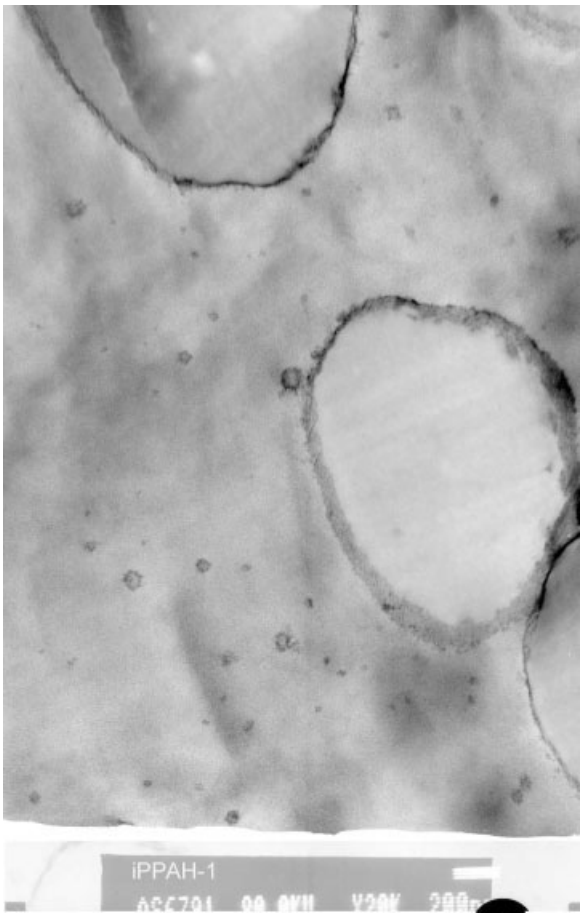

Figure 8 TEM micrograph of iPPAH1 (28 wt % PS, Φ = 30%); scale bar 200 nm.

result in appreciable change in both T_1 and $T_{1\rho}$ values, confirming that only minor changes in the morphology have taken place upon melt processing. The relaxation times measured by solid-state NMR represent an "average" property of the samples and clearly confirm, on a more general level, those already outlined when discussing the SEM and TEM images.

To further improve the stability of the morphology upon melt processing a "new" approach has

TABLE II
Solid-State NMR Relaxation Times

Sample	T_1 {PP} (s)	$T_{1\rho}$ {PP} (ms)	T_1 {PS} (s)	$T_{1\rho}$ {PS} (ms)
PP	1.1			
PS			3.5	
iPPA/PS 70/30	1.2	36	2.8	12
iPPAH2 (before processing)	1.0	37	1.5	14
iPPAH2 (after processing)	1.2	46	2.5	13
iPPAH3 (before processing)	1.2	51	1.4	15
iPPAH3 (after processing)	1.1	50	1.2	16
iPPAH6 (before processing)	1.2	37	1.2	7
iPPAH6 (after processing)	1.2	56	1.1	10

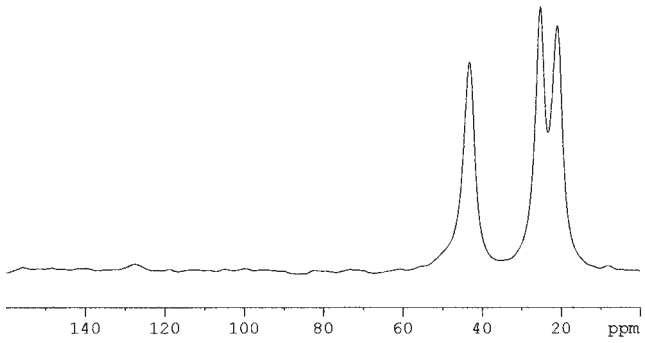

Figure 9 Solid-state NMR spectrum of sample iPPAH3 (T_1 determination via cross-polarization).

tentatively been followed. Grafting of styrene onto iPP was carried out in the presence of DVB as crosslinking agent. According to the general mechanism accepted in the literature (Fig. 10), the presence of DVB should lead to the formation of a network structure in the PS phase, which should then hinder the coalescence between PS particles upon melting due to an increased viscosity of the dipersed phase. The morphology of the processed materials (TEM pictures of iPPAH5 and iPPAH8 are reported as an example in Fig. 11) shows indeed the presence of very small (100 nm) PS domains. At a closer look (Fig. 12), however, two different kinds of morphologies seem to coexist in the same sample. The first one consists of a PP matrix in which the PS domains, whose dimensions can reach the order of micrometers, are dispersed. In the second one (Fig. 12, inset) the PS phase seems to constitute a kind of network in which the PP phase is entrapped. A possible explanation of these results may be found in the fact that the crosslinked PS, when processed, actually retains its three dimensional network structure and does not flow. In this way the PP is able, upon processing, to fill the network cells.

The presence of such types of structure should however influence the crystallization behavior of iPP. Indeed the DSC traces (Fig. 13) clearly show that the one-step crystallization of iPP (for example in iPPAH2) does not occur anymore when processing samples containing DVB. Instead, a two-step crystallization is observable, probably due to the presence of constrained and unconstrained iPP in the same sample. Independently of the structure formed, it must be outlined that the size of the PS domains remains unchanged upon processing. This is also confirmed by the solid-state NMR data (last two rows of Table II). The T_1 values of the two components are remarkably close both before and after processing while the $T_{1\rho}$ values remain different, thus suggesting that the two polymers are intimately mixed but still separated at the nanometer scale. It must be finally outlined that actually the $T_{1\rho}$ values for the same com-

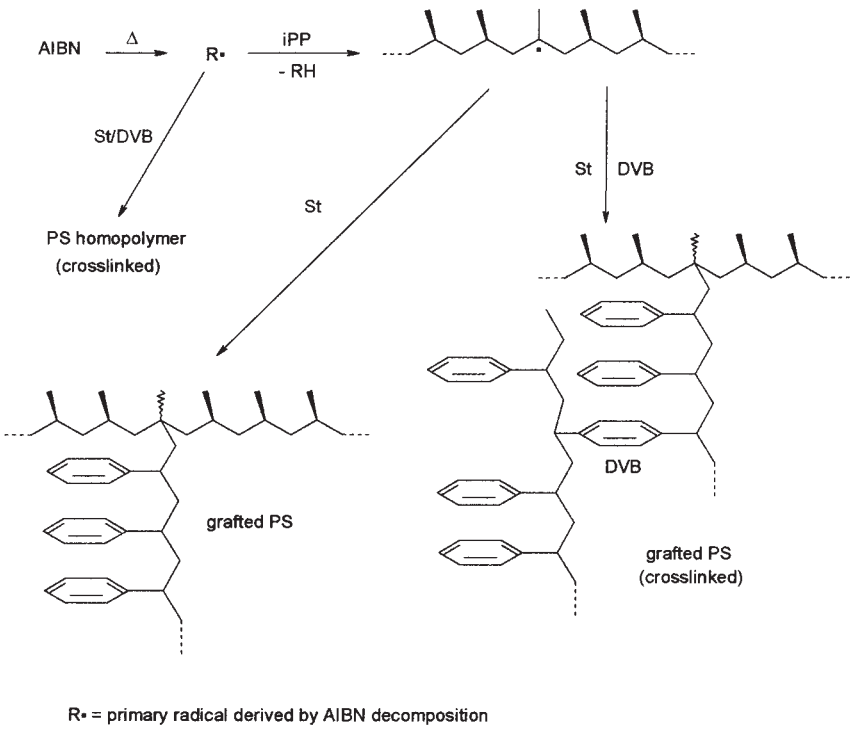

Figure 10 Graft polymerization of St/DVB mixture: simplified mechanism (transfer reactions from the growing chains are not displayed for simplicity).

ponent are not the same before and after processing, contrary to what is observed for the materials that do not contain DVB. This may constitute indirect evidence that, in the former case, a "new" kind of microseparation between PP and PS actually takes place upon processing.

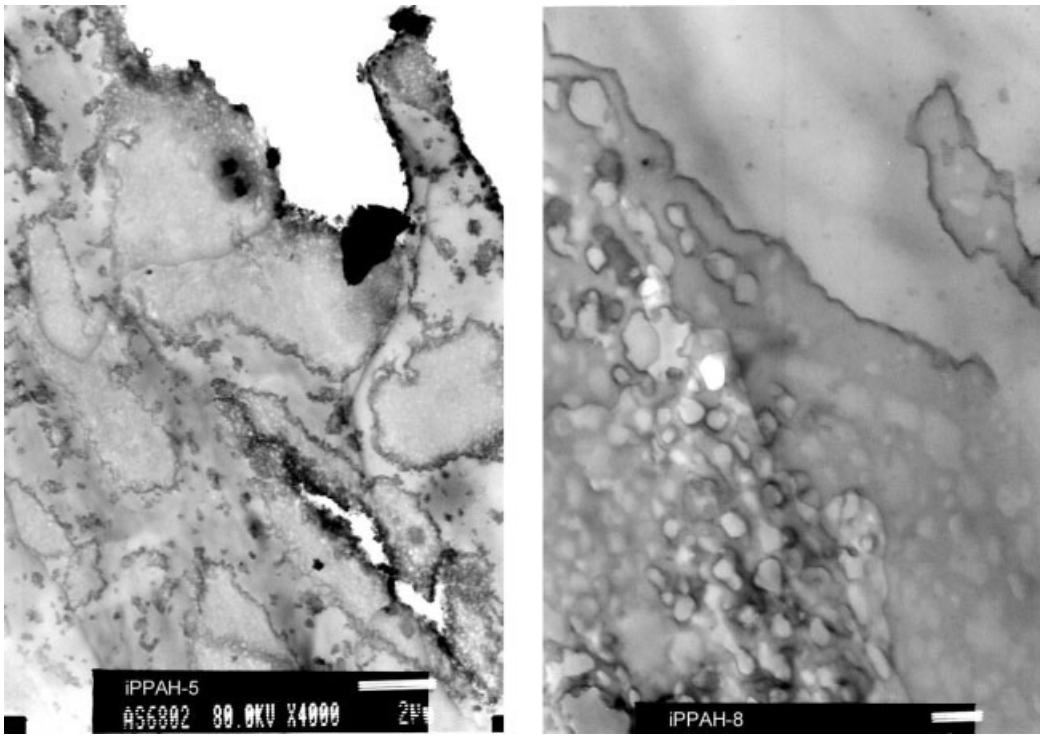

Figure 11 TEM images of iPPAH5 (scale bar 2 μm) (a) and iPPAH8 (scale bar 500 nm) (b).

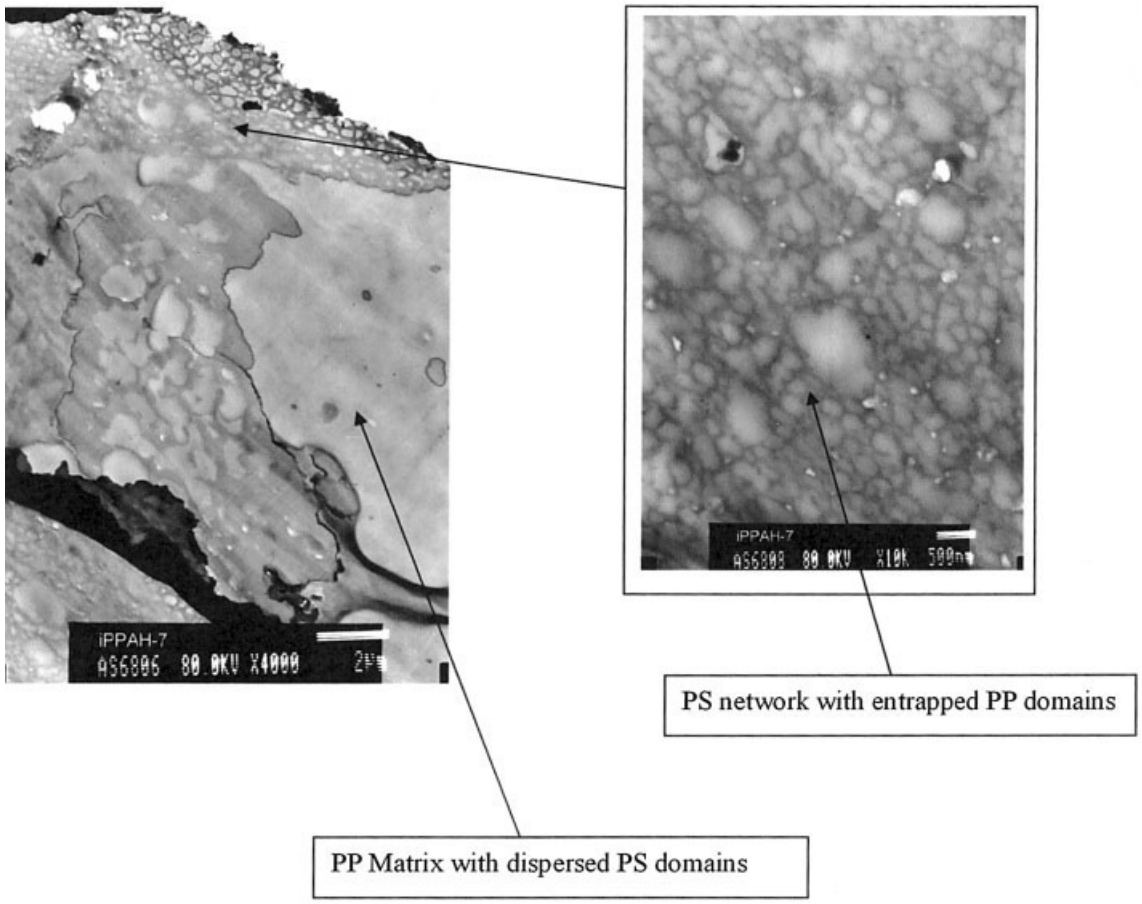

Figure 12 TEM micrographs of iPPAH7; scale bars 2 μm and 500 nm.

CONCLUSION

iPP/PS blends prepared via solid-state grafting of styrene onto iPP have been processed in the melt and their morphology compared with physical iPP/PS blends. The starting morphology, constituting PS domains size of about 50 nm, is in general not stable during melt processing. Formation of larger PS domains is usually observed probably due to the coalescence of the free PS domains present in the starting material. Stabilization of the morphology has been attempted by increasing the grafting efficiency and by crosslinking the PS domains.

Decreasing the PS content represents a good method for avoiding coalescence but its applicability is clearly limited by the restriction in composition.

Solid-state polymerized blends with high values of the grafting efficiency can be obtained but the stability of their morphology is actually only partial. Coalescence of the PS domains is still taking place even if to a lesser extent, resulting in a bimodal distribution of the PS domain size. One population of PS domains retains the original size (50–100 nm) and the other increases in size up to 300 nm. Even within this limit, the morphology is much finer than that of physical iPP/PS blends and is at least comparable to what is oberved when iPP and PS are blended in the presence of a compatibilizer.[1,30–33]

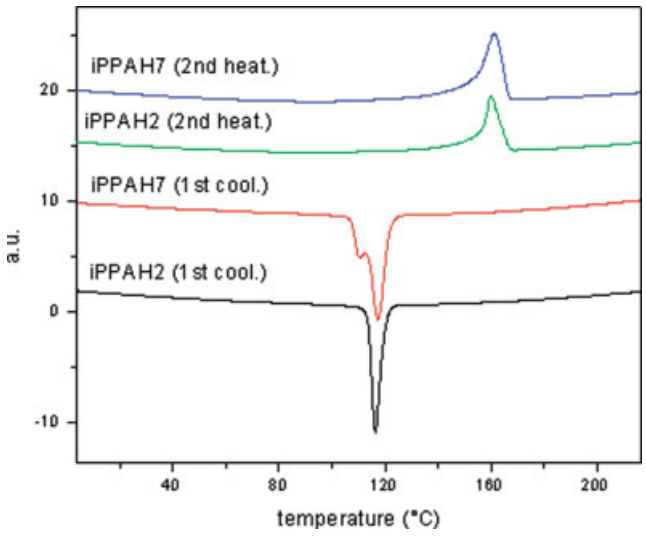

Figure 13 DSC traces for iPPAH7 and iPPAH2.

Crosslinking of the PS domains resulted, after melt processing, in the formation of a complex morphology. The crosslinked PS does not give coalescence but forms a network in which the iPP is entrapped. On the other hand, the uncrosslinked PS forms small domains dispersed in an iPP matrix.

The three methods mentioned above are effective, within the outlined limits, in stabilizing the starting morphology. Their effect on the rheological and mechanical properties of the blends is currently under investigation.

H. Repin (DSM Research), W. Bruls (DSM Research), F. op den Buijsch (DSM Research), and J. D. van Loon (Basell) are acknowledged for the very helpful discussions. P. Magusin and E. M. van Oers are especially acknowledged for the help in the solid-state NMR experiments. A. B. Spoelstra and P. Schmit are acknowledged for the TEM and SEM measurements, respectively.

References

1. Adewale, A. A.; DeNicola, A.; Gogos, C. G.; Mascia, L. Adv Pol Tech 2000, 19, 180.
2. Rätzsch, M.; Bucka, H.; Wohlfahrt, C. Angew Makromol Chem 1995, 229, 145.
3. Rätzsch, M.; Bucka, H.; Hesse, A.; Arnold, M. J Macromol Sci: Pure Appl Chem 1996, A33, 913.
4. Galli, P. J Macromol Sci: Pure Appl Chem 1999, A36, 1561.
5. Galli, P. Macromol Symp 1994, 78, 269.
6. Galli, P. Prog Polym Sci 1994, 19, 959.
7. Galli, P.; Haylock, J. C.; Albizzati, E.; DeNicola, A Macromol Symp 1995, 98, 1309.
8. Galli, P. J Macromol Sci: Phys 1996, B35, 427.
9. Galli, P.; Collina, G.; Sgarzi, P.; Baruzzi, G.; Marchetti, E. J Appl Polym Sci 1997, 66, 1831.
10. Galli, P. J Macromol Sci: Pure Appl Chem. 1999, A36, 1797.
11. DeNicola, A. J.; Guhaniyogi, S. EP Patent EP0439079 A2, 1991.
12. Galli, P.; DeNicola, A. J.; Smith, J. A. EP Patent EP0437808 (1991).
13. Ferraro, A.; Fava, R. A.; Van Every, K. W. Compalloy '93 1993, 71.
14. Giroux, T. A.; Song, C. Q. Polym Prepr 1999, 40, 130.
15. Song, C. Q.; Giroux, T. A. Polym Prepr 1999, 40, 110.
16. Rätzsch, M.; Hesse, A.; Bucka, H. DE Patent DE4435534 (1996).
17. Rätzsch, M.; Hesse, A.; Bucka, H. US Patent US5585435 (1996).
18. Panzer, U.; Bucka, H.; Hesse, A.; Rätzsch, M.; Reichelt, N. EP Pat. EP0792894 (1997).
19. Rätzsch, M.; Hesse, A.; Bucka, H.; Reichelt, N.; Panzer, U. DE Patent DE19607430 (1997).
20. Reichelt, N.; Panzer, U.; Hesse, A.; Bucka, H.; Rätzsch, M. EP Patent EP0879830 (1998).
21. Reichelt, N.; Rätzsch, M.; Heikin, S.; Ivanchev, S.; Mesh, A.; Fodorova, N. EP Patent EP0964011 (1999).
22. DeNicola, A. J.; Fava, R. A. Polym Mater Sci Eng 1997, 76, 162.
23. Roelands, D. Graduation Report, Eindhoven University of Technology, The Netherlands, 1999.
24. DeNicola, A. J.; Guhaniyogi, S. EP Patent EP0439079 A2 (1991).
25. Picchioni, F.; Goossens, J. G. P.; van Duin, M.; Magusin, P. J Appl Polym Sci, to appear
26. Montezinos, D.; Wells, B. G.; Burns, J. L. J Polym Sci: Polym Lett Ed 1985, 23, 421.
27. Trent, J. S.; Scheinbeim, J. I.; Couchman, P. R. Macromolecules 1983, 16, 589.
28. Schmidt-Rohr, K.; Spiess, H. W. Multidimensional Solid-State NMR and Polymers; Academic Press: London, 1994.
29. Simonutti, R.; Mariani, A.; Sozzani, P.; Bracco, S.; Piacentini, M.; Russo, S. Macromolecules 2002, 35, 3563.
30. D'Orazio, L.; Guarino, R.; Mancarella, C.; Martuscelli, E.; Cecchin, G. J Appl Polym Sci 1997, 65, 1539.
31. Radonjič, G.; Musil, V.; Šmit, I. J Appl Polym Sci 1998, 69, 2625.
32. Syed Mustafa, S. J.; Nor Azlan, M. R.; Ahmad Fuad, M. Y.; Mohd Ishak, Z. A.; Ishiaku, U. S. J Appl Polym Sci 2001, 82, 428.
33. Raghu, P.; Nere, C. K.; Jagtap, R. N. J Appl Polym Sci 2003, 88, 266.